Construction and Building Materials 151 (2017) 147–157

Contents lists available at ScienceDirect

Construction and Building Materials

journal homepage: www.elsevier.com/locate/conbuildmat

Compressive stress distribution in prestressed concrete and its effect on railroad crosstie design

Zhengboyang Gao, Yu Qian *, Marcus S. Dersch, J. Riley Edwards

Rail Transportation and Engineering Center – RailTEC, Department of Civil and Environmental Engineering, University of Illinois at Urbana-Champaign, 205 N. Mathews Ave., Urbana, IL 61801, United States

HIGHLIGHTS

- Compressive stress distribution in concrete crossties is captured.
- The rail seat load magnitude and the distribution angles have a direct relationship.
- The distribution angles are sensitive to changes in support conditions.
- Stress distribution behavior can affect the mechanical design of concrete crossties.

ARTICLE INFO

Article history:
Received 22 August 2016
Received in revised form 8 May 2017
Accepted 21 May 2017

Keywords:
Concrete
Railroad crossties
Railroad sleepers
Stress distribution
Support conditions
Bending moments
Finite-element modeling

ABSTRACT

Recently, track mileage with concrete crossties has been increasing throughout the world. In North America, for example, approximately 30 million crossties are currently in service on Class I freight railroads. It is essential to understand the concrete crosstie bearing capacity and flexure behavior for both design and safety purposes. The American Railway Engineering and Maintenance-of-Way Association (AREMA) Recommended Practices and Australian Standard's (AS) current flexural design methodologies consider rail seat loads to be vertically transferred to the neutral axis. However, the International Union of Railways (UIC) assumes rail seat loads are distributed at a 45 degree angle to the neutral axis. This load distribution behavior is commonly seen in the design of concrete corbels and spread footings, but is not well documented in the design of concrete crossties, and different assumptions (i.e. in AREMA and UIC design methods) will result in different designs. Better understanding the load distribution in concrete crossties will help to improve the design of concrete crossties and optimize their performance. This study presents preliminary results from an on-going research project at the University of Illinois at Urbana-Champaign (UIUC) focused on concrete crosstie mechanical behavior. A parametric study using three-dimensional (3D) finite element modeling (FEM) was performed to investigate stress distribution below the rail seat and quantify the corresponding distribution angles in prestressed concrete crosstie under static wheel loading. Laboratory experiments were also performed and successfully validated the results obtained from the numerical simulations. The results from both numerical simulation and laboratory experiments indicate the stress distribution angle under rail seat is not constant which disagrees with the assumptions in UIC 713R. Moreover, the stress distribution angle under rail seat is found to be sensitive to crosstie support conditions, and its value follows a direct relationship with rail seat load magnitude. The findings from this study can help to optimize prestressed concrete crosstie bearing capacity design.

1. Introduction

The primary purposes of crossties are to provide support for the rail, maintain track geometry, and distribute wheel loads to the ballast [1]. Timber is the most commonly used material for crossties in the United States, constituting around 90–95% of the crossties in service [2]. The remaining 5–10% is mostly made up of concrete. The application of steel and composite crossties has increased in recent years, but their share in the market is still negligible. Nowadays, the installation of concrete crossties in North America is increasing, especially for heavy-haul freight railroad lines [3].

* Corresponding author.
E-mail addresses: zgao9@illinois.edu (Z. Gao), yuqian1@illinois.edu (Y. Qian), mdersch2@illinois.edu (M.S. Dersch), jedward2@illinois.edu (J.R. Edwards).

http://dx.doi.org/10.1016/j.conbuildmat.2017.05.186
0950-0618/

An international survey conducted by researchers at the University of Illinois at Urbana-Champaign (UIUC) in 2012 found that crosstie cracking from center binding was ranked as the third most critical issue with concrete crossties [4]. However, the survey results indicated that rail seat positive cracks were not an issue in the field. Even though rail seat deterioration (RSD) is recognized as one of the most common failure modes, the rail seat cracks caused by loading are rarely detected in the field, indicating that the rail seat sections in concrete crossties may be overdesigned. The objective of this study is to analyze how rail seat loads are transferred inside prestressed concrete crossties and compare the load path with assumptions made in different design methodologies to evaluate their accuracy.

1.1. Overview of current design methodologies

The structural design of concrete crossties is primarily based on estimating the flexural demand a crosstie is expected to be subjected to within the rail seat and the center region (shown in Fig. 1) [5]. At both the rail seat and crosstie center, positive bending moments, defined as the crosstie being concave downwards, and negative bending moments, defined as the crosstie being concaved upwards, need to be calculated in the design process. The American Railway Engineering and Maintenance-of-Way Association (AREMA) [6], Australian Standard (AS) [7], and International Union of Railways (UIC) [8] each have their own design recommendations/standards. These standards consider the crosstie to be linear-elastic and include crosstie length, crosstie spacing, axle load, train speed, and a safety factor in their design methods. The center bending moment is calculated by modeling the crosstie as a cantilevered beam fixed at the crosstie center, while the rail seat bending moment is calculated by modeling the crosstie as a cantilevered beam fixed at the rail seat center.

Both AREMA Chapter 30 and AS 1085.14, the chapters on prestressed concrete crossties, consider rail seat loads as concentrated point loads acting at the center of rail seats. To calculate the rail seat bending moment (M_{RS+}), AREMA assumes the support condition to be a fully uniform support condition, where the reaction is uniformly distributed across the entire crosstie (Fig. 1(a)), whereas AS assumes a newly tamped support condition, with the uniform ballast reaction acting symmetrically about the rail seat load (Fig. 1(c)). To calculate the center bending moment (M_{C-}), AREMA assumes a partially consolidated support condition, where the reaction within the center region is reduced 39% (Fig. 1(b)), while AS assumes a fully uniform support condition (Fig. 1(d)).

UIC 713R assumes rail seat loads to be uniformly distributed along the entire width of the rail seat, rather than a concentrated point load. Similar to AS, UIC uses the newly tamped condition to get the rail seat bending moment (Fig. 1(e)), and the uniform support condition for calculating the center bending moment (Fig. 1(f)). Unlike other standards, UIC 713R assumes the rail seat load to be distributed uniformly at a 45 degree angle to the neutral axis of the crosstie as illustrated in Fig. 2.

Considering the given support conditions and the varying rail seat load and load path assumptions shown in Fig. 1, different rail seat bending moment values are calculated. Fig. 3 shows the design rail seat bending moment for a 102 in. (259 cm) long, 9.5 in. (24 cm) deep crosstie with a 6 in. (15 cm) rail base subject to a 62.1 kip (276 kN) factored high-impact rail seat load under the various load path assumptions shown in Fig. 1. When the rail seat load is assumed to act over the entire width of the rail base, there is a 47 kip-in (5.3 kNm) reduction in rail seat bending moment (from 326 kip-in (36.8 kNm) to 279 kip-in (31.5 kNm)) when compared to the moment found assuming the rail seat acts as a point load. A 69 kip-in (7.8 kNm) reduction can also be seen in this bending moment (from 279 kip-in (31.5 kNm) to 210 kip-in (23.7 kNm)) when the UIC assumption is used and the rail seat load is distributed at a 45 degree angle from the rail base. As mentioned previously, rail seat cracking is rarely seen in the field, which implies that current concrete crossties could be overdesigned at rail seat regions due to over-conservative assumptions about the flow of forces in the crosstie rail seat sections. To investigate further, a finite element (FE) modeling approach was used to evaluate the stress distribution below rail seats. Laboratory experimentation was also conducted to ensure the FE model captured the true behavior of prestressed concrete crossties. The distribution angles were quan-

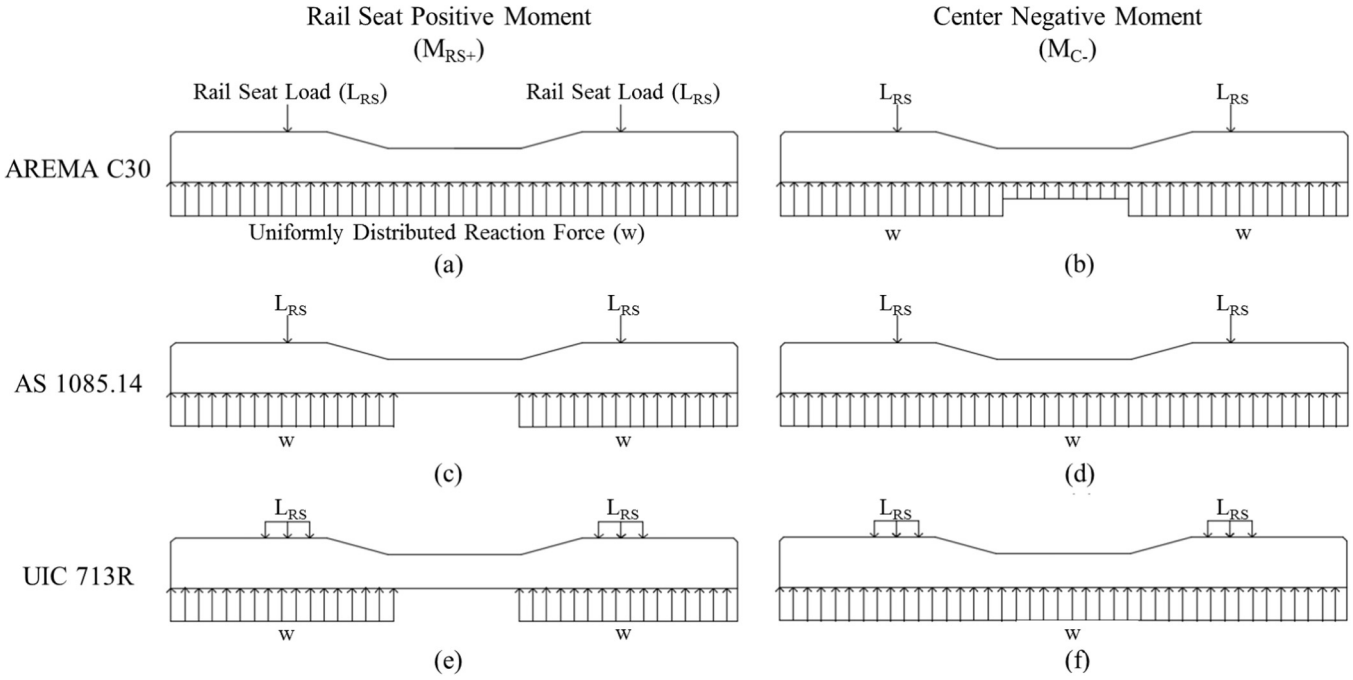

Fig. 1. Support conditions for selected design recommendations: (a) AREMA M_{RS+}, (b) AREMA M_{C-}, (c) AS M_{RS+}, (d) AS M_{C-}, (e) UIC M_{RS+}, (f) UIC M_{C-} (5).

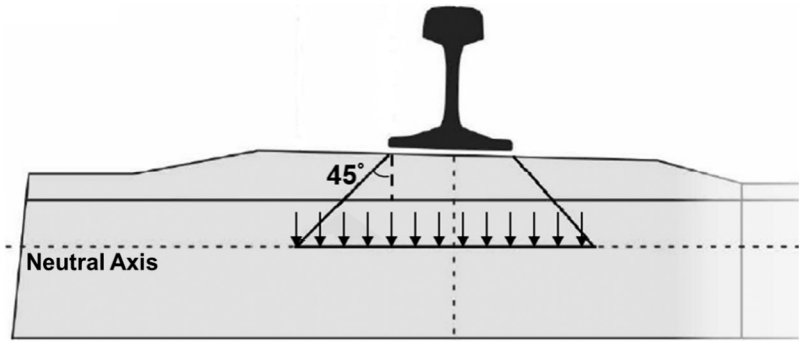

Fig. 2. Profile view of half of a crosstie and load distribution under rail seat according to UIC 713R.

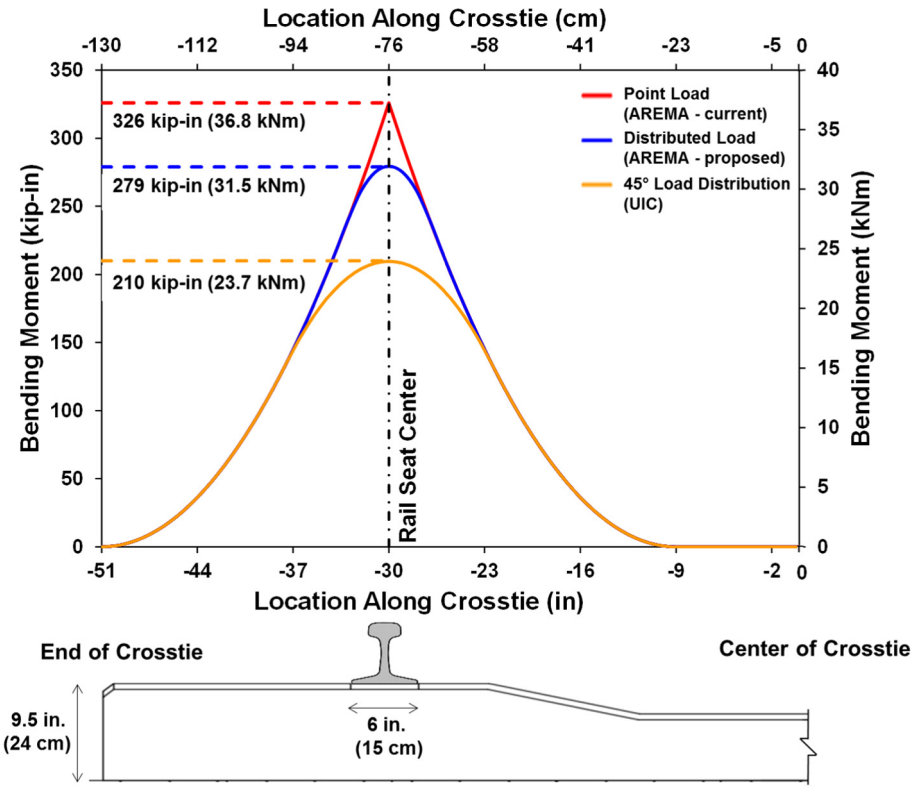

Fig. 3. Rail seat bending moment with different load path assumptions (102 in. (259 cm) crosstie length, 9.5 in. (24 cm) crosstie depth, 6 in. (15 cm) rail base width, 62.1 kip (276 kN) rail seat load).

tified through sensitivity analysis and were then compared with UIC 713R assumptions. Evaluations on different crosstie design methodologies regarding their estimated flexural capacity were drawn from the FE results.

2. Finite-element (FE) modeling

The finite-element (FE) model of a prestressed concrete crosstie and a ballast block was developed using ABAQUS, a commercially available FE modeling software. An overview of the FE model is shown in Fig. 4. The geometry and properties of the crosstie model were based on a concrete crosstie that is often used in North American heavy haul freight tracks. The crosstie length and width are 102 in. (259 cm) and 11 in. (28 cm) respectively, and it has a depth of 9.5 in. (24 cm) [9]. 20 prestressed steel wires were modeled as truss elements and embedded inside the concrete. However, due to proprietary reasons, the pattern of the steel wire arrangement is not shown in Fig. 4. Rail cant, as shown in Fig. 4(a), is a standard design feature of concrete crossties for many suppliers. The main purpose of the rail cant is to reduce the wear at the wheel-rail interface. Using the concept of the Extended Drucker-Prager modeling, a technique for developing pressure-dependent plasticity models suitable for simulating granular and frictional materials, generic ballast block was attached beneath the crosstie model to represent the support condition [10]. The ballast block was modeled to be plastic, with a constant Young's Modulus, Poisson's ratio, and yield strength. The material properties of all components within the FE model are shown in Table 1. By rearranging the geometry of the ballast block, the crosstie model could experience different support conditions. Rail seat load was distributed vertically and uniformly over a 6 in. (15 cm) by 7 in. (18 cm) area (common dimensions of rail pads) at each of the two rail seat regions.

The loading sequence of the FE analysis consisted of three steps. In the first step, a prestress force of 7 kips (31 kN) was applied to

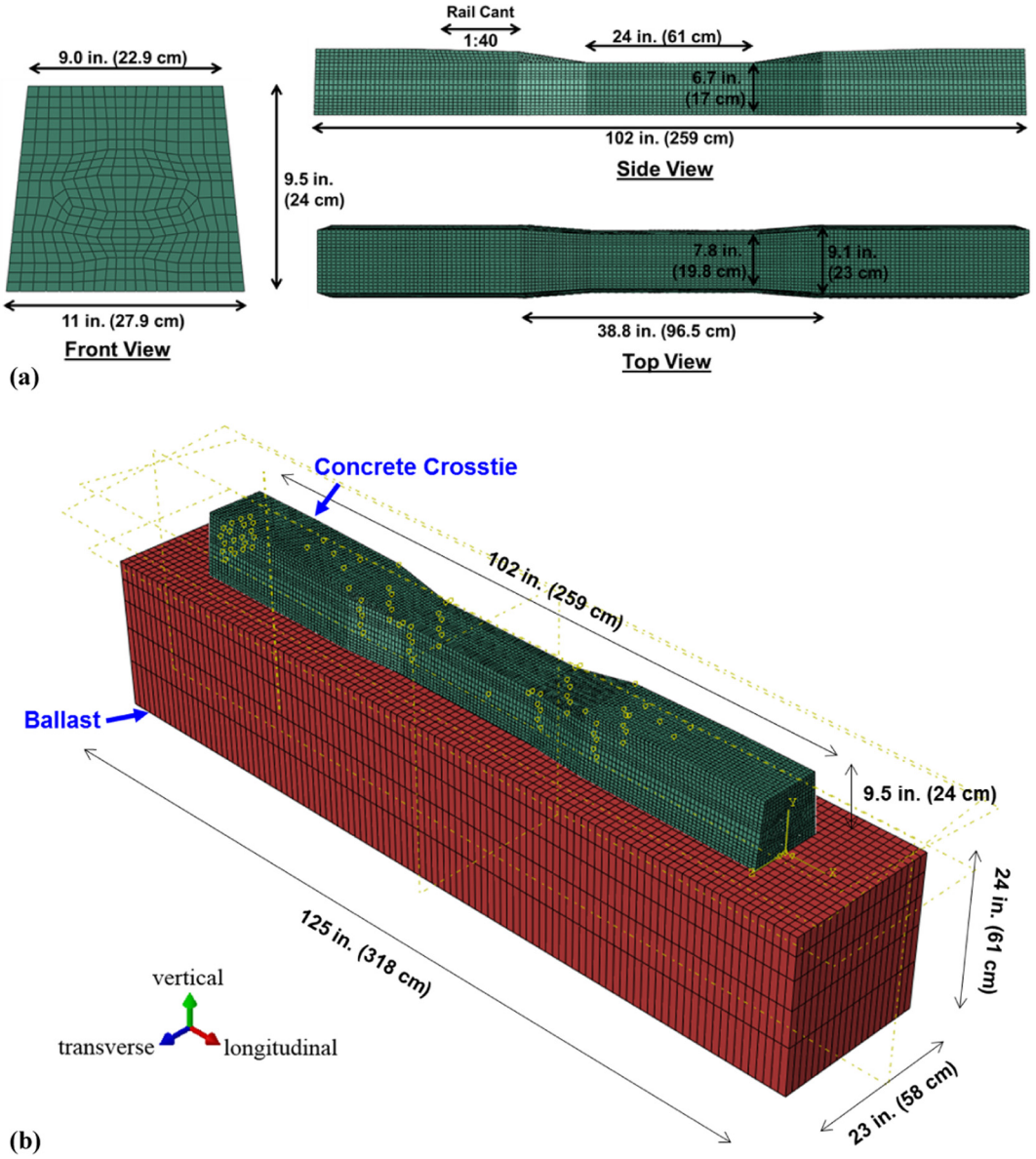

Fig. 4. Finite-element model setup (a) three-view drawing of the crosstie model, (b) isometric view of the crosstie model and ballast block.

Table 1
Material properties of all components [11].

Component	Element Type	Unit Weight, lb/ft^3 (kg/m^3)	Young's Modulus, ksi (GPa)	Poisson's Ratio	Yielding Strength, ksi (GPa)	Friction Coefficient*
Steel Wire	Truss	489 (7833)	32,382 (223)	0.30	255 (1.8)	N/A
Concrete	Solid Homogeneous	150 (2400)	4347 (30)	0.20	N/A	N/A
Ballast	Solid Homogeneous	100 (1613)	30 (0.21)	0.30	0.058 (0.00040)	0.50

* Note: friction coefficient was only defined at the interaction between the crosstie and the ballast.

each of the 20 steel wires while the crosstie was fixed at the center, so that no movement in any direction was allowed. In the second step, the initial boundary condition was removed and the prestress force was gradually released. Vertical rail seat loads were applied in the third and final step while the center cross sections of the crosstie, in both the longitudinal and transverse directions, were confined. For the center cross section in the longitudinal direction, only rotation in the longitudinal direction and displacements in the vertical and transverse directions were allowed (Fig. 5(a)); for the center cross section in the transverse direction, rotation in the transverse direction and displacements in the vertical and longitudinal directions were permitted (Fig. 5(b)). These boundary conditions were considered to be consistent with the true crosstie behavior expected in the field. The reason behind these boundary

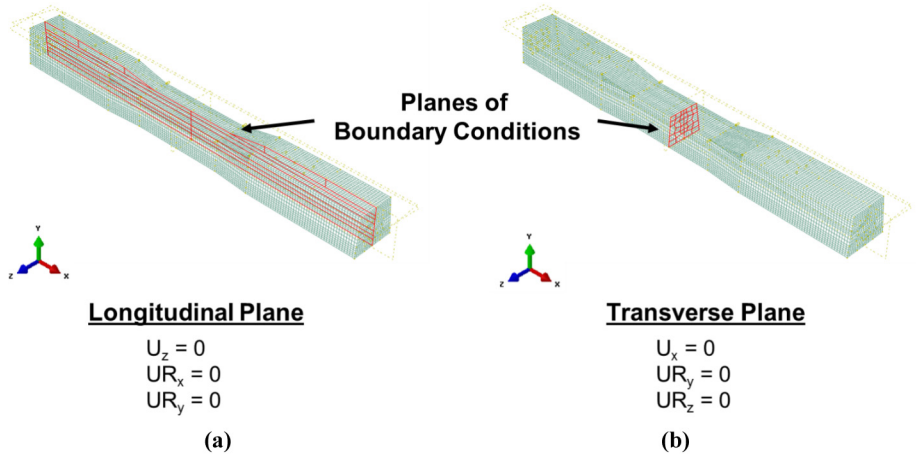

Fig. 5. Boundary conditions under loading: (a) at longitudinal plane, (b) at transverse plane (U = displacement, UR = rotation).

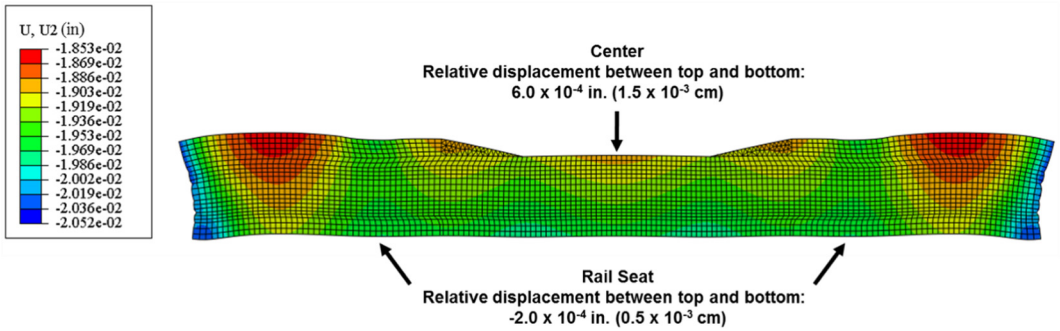

Fig. 6. Crosstie's amplified deformed shape under "full support" condition (deformation scale factor: 500).

conditions is that when symmetric loading and support are applied, the crosstie can only be expected to move or rotate symmetrically with respect to the center cross section.

Fig. 6 illustrates the vertical displacement along the length of the crosstie with respect to the base of the ballast and its amplified deformation after a 20 kip (89 kN) rail seat load was applied at both rail seats under "full support" condition, which means that the bottom of the concrete crosstie was in full contact with the ballast. It is important to note that unlike the assumptions made by AREMA, AS, or UIC, the "full support" condition did not necessarily imply that the ballast reaction force was uniform within the entire contact area as shown in Fig. 1(f). The results corresponded closely with the behavior that is typically seen in the laboratory and in the field [12], and since the crosstie was only loaded vertically at the rail seats, the entire crosstie moved down. However, the amplified deformed shape and the relative displacements between top and bottom of the crosstie indicate that the center region experienced negative bending, and the rail seat sections experienced positive bending.

Compressive stress was concentrated right under the two rail seats, and spread through the crosstie's neutral axis located along the geometric centerline of the crosstie. Fig. 7(b) shows a zoomed-in pressure distribution diagram of the left rail seat section of the crosstie (highlighted square section in Fig. 7(a)). The pressure contour map looks similar to Boussinesq's distribution for soil under concentrated load [13]. The reasons behind the similarity are threefold. First, Boussinesq's theory assumes soil to be elastic and isotropic, both of which also held true for the FE model. Second, the applied load is vertical, concentrated acting on the surface for both cases. Third, Hooke's law applies for soil mass under Boussinesq's theory and concrete, that is, the ratio between stress and strain remains constant. However, Boussinesq's theory assumes soil to be homogeneous, semi-infinite, and weightless, none of which are valid assumptions for concrete. Moreover, it is possible that the pressure distribution may look different for cracked concrete crossties, given the stress at the cracked regions will be zero.

Vertical load along the neutral axis is typically used for calculating the bending moments along the crosstie [6–8]. Therefore, understanding the vertical load distribution along the neutral axis is important for quantifying crosstie bending behavior. Fig. 7(c) shows the vertical load distribution diagram under the left rail seat section (highlighted square section in Fig. 7(a)). To quantify the distribution of compressive stress below the rail seat, distribution angles were calculated. To compare the FE results with the assumptions made by UIC 713R, the same practice was used to define the distribution angles. As can be seen in Fig. 7(d), lines were drawn between the ends of the rail seat and the points on the neutral axis where the majority of the compressive stress (over 99%) ceased to distribute. The distribution angles were defined as the angles between the inclined lines and the vertical reference lines. For this particular case, the distribution angle at the field side, θ_f, was 31.1 degrees, and the distribution angle at the gauge side, θ_g, was 23.6 degrees.

To ensure the values of the distribution angles captured the actual behavior of concrete crossties, and did not depend on the mesh density, four tests with different crosstie mesh densities were completed and the corresponding θ_f and θ_g were collected. The number of elements associated with the four mesh densities and the angle values are shown in Table 2, as well as the absolute

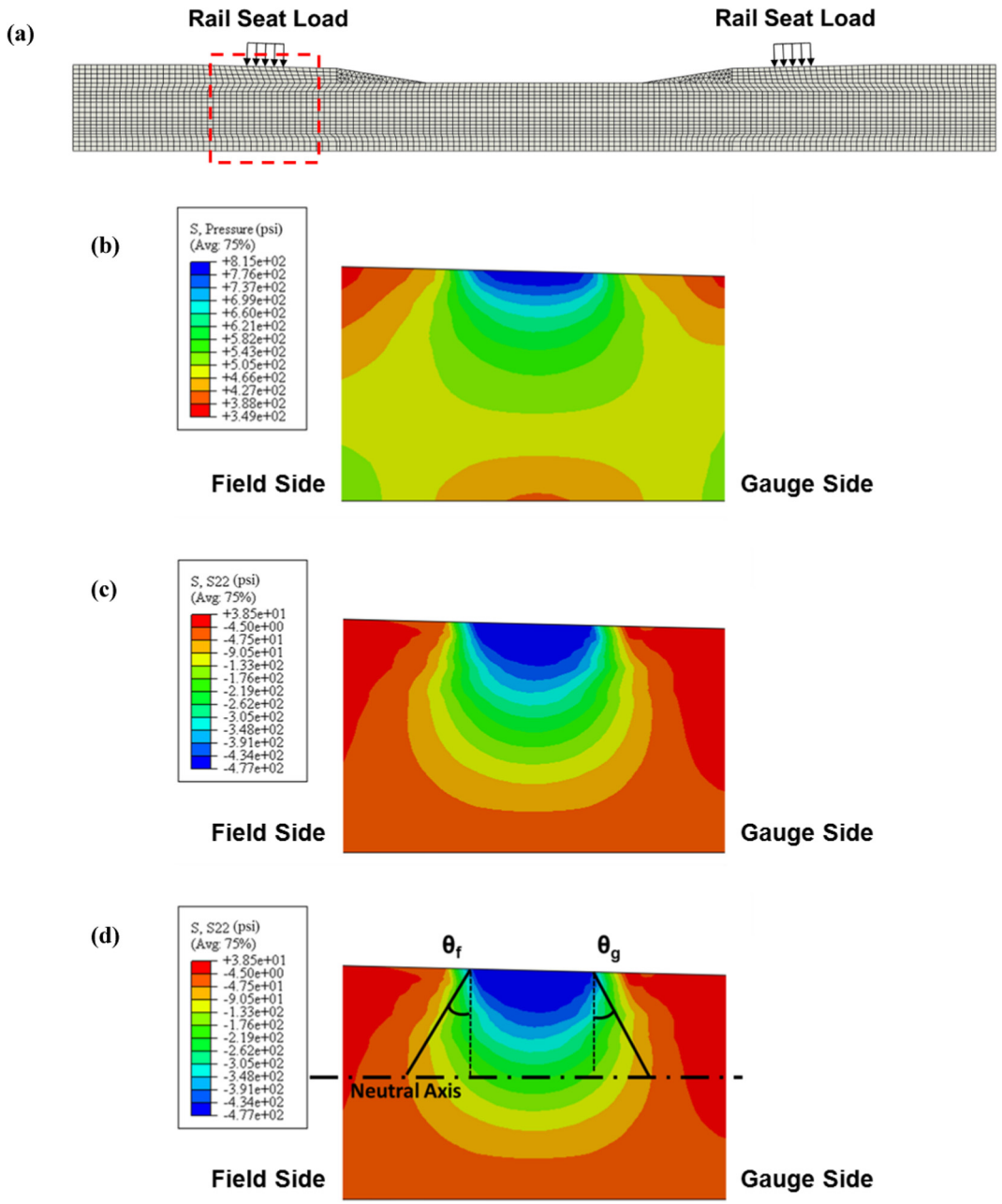

Fig. 7. Zoomed-in rail seat section: (a) location of the cross section, (b) pressure distribution, (c) vertical stress distribution, (d) vertical stress distribution with distribution angles specified.

Table 2
Effect of mesh density on angle values.

Number of Elements	θ_f (°)	Absolute Percent Difference (%)	θ_g (°)	Absolute Percent Difference (%)
9428	21.2	N/A	14.2	N/A
11,416	34.7	63.7	21.0	47.9
53,422	31.1	10.4	23.6	12.4
91,124	30.8	1.0	24.3	3.0

percent difference between angles. The absolute percent difference was defined as the ratio of the absolute difference between angle values in two neighboring mesh cases to the angle value in the preceding mesh case. As can be seen in Table 2, the absolute percent difference decreased, as the number of elements increased, and it was believed that the difference between 53,422 elements and 91,124 elements was relatively minimal (1.0% absolute difference for θ_f and 3.0% difference for θ_g); however, it usually took more than triple the time to complete a test with 91,124 elements as compared to a test with 53,422 elements. Therefore, to save computation time, while maintaining accuracy, the crosstie mesh of 53,422 elements was used in the remaining tests.

3. Model validation

To validate the FE model, laboratory experimentation was performed by Rail Transportation and Engineering Center (RailTEC) at UIUC. Experimentation was conducted at the Research and Innovation Laboratory (RAIL) housed within the Harry Schnabel, Jr. Geotechnical Engineering Laboratory. The same type of prestressed concrete crosstie that the FE model was based on was used in this experiment. A 6 in. (15 cm) by 9 in. (23 cm) plastic frame consisting of two strain gauges (Fig. 8(a)) was attached to the intermediate vertical layer of the prestressing wires right below the rail seat before the concrete was poured inside the form, such that the strain gauges would be embedded into the concrete in a vertical orientation to capture vertical compressive strains when rail seat loads were applied (Fig. 8(b)) [14]. The wires connected to the gauges were extended outside of the crosstie and were plugged into a National Instruments (NI) 9235 module [15]. A NI compact data acquisition system (cDAQ) 9174 was used to output the strain data. The location of the strain gauges within the crosstie can be seen in Fig. 8(c).

The Static Load Testing Machine (SLTM) at RAIL was used to apply static rail seat loads to the crosstie (Fig. 9). Equal static loads up to 20 kip (89 kN) were applied simultaneously at both rail seats. Rubber pads were placed continuously along the bottom of the crosstie to simulate the ballast support condition. Previous research at RailTEC has proven that the stiffness of the rubber pads was comparable to the ballast stiffness typically seen in the field [12]. Strain data were collected as the rail seat loads increased from 0 to 20 kip (89 kN), and during the process, no crack was observed on the crosstie.

Vertical strain data were gathered from the FE model at the same locations as the embedded strain gauges after tests were completed under rail seat loads ranging from 5 kip (22 kN) to 20 kip (89 kN). Fig. 10 shows the comparisons between data from laboratory experimentation and from the FE model. As can be seen in the graph, the differences between the two sets of data were minimal. To be more specific, the smallest absolute percent difference between the correlated values was less than 0.1%, and the largest absolute percent difference was around 10%. Furthermore, for both strain gauge data and FE results, the compressive strains near the gauge side were always larger than those near the field side. The authors were comfortable with the minimal variance between laboratory data and FE results; thus, the FE model was considered to be capable of predicting and measuring the compressive behavior of the concrete crosstie.

4. Parametric study

In order to quantify distribution angles and investigate the factors that could affect their magnitudes, a parametric study was conducted. The parametric study addressed two objectives. The first objective was to quantify the relation between distribution angles of compressive stress and varying magnitudes of rail seat loads with a given ballast support condition. The second objective was to quantify the relation between distribution angles and varying support conditions with a given rail seat load magnitude. Loads at both rail seats were equal, as asymmetric loading was not considered in the study.

4.1. Effect of rail seat load magnitude on distribution angle

Based on the recommendations provided within Chapter 30 of the AREMA Manual on Railway Engineering [6], the design rail seat load is calculated using the following equation:

$$R = WL \times DF \times (1 + IF)$$

where,

R = design rail seat load (kip)
WL = unfactored wheel load (kip)
DF = distribution factor (from AREMA Figure 30-4-1)
IF = impact factor (specified to be 200% by AREMA)

For loaded freight cars in North America, the 95th percentile vertical wheel load is 40 kip (178 kN) [6]. With the most commonly seen crosstie spacing of 24 in. (61 cm), the distributed factor is found to be approximately 50% [6]. The static rail seat load is then set to be 20 kip (89kN) without the impact factor. However, AREMA uses 62.1 kip (276 kN) as the design rail seat load for cal-

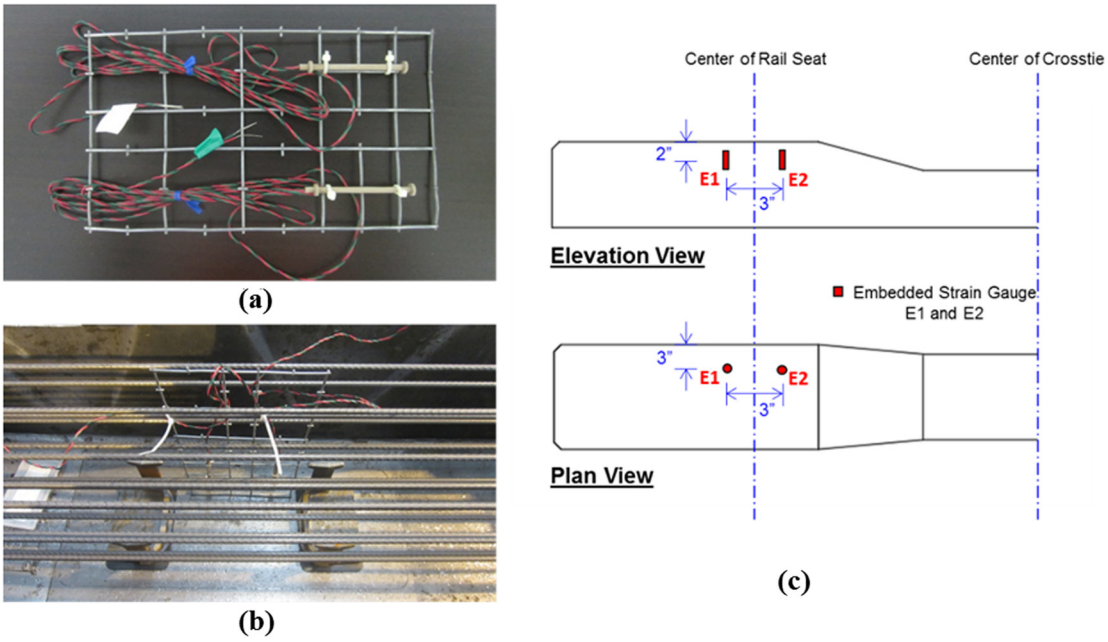

Fig. 8. Embedded strain gauges: (a) frame, (b) installation before concrete pouring, (c) installation locations.

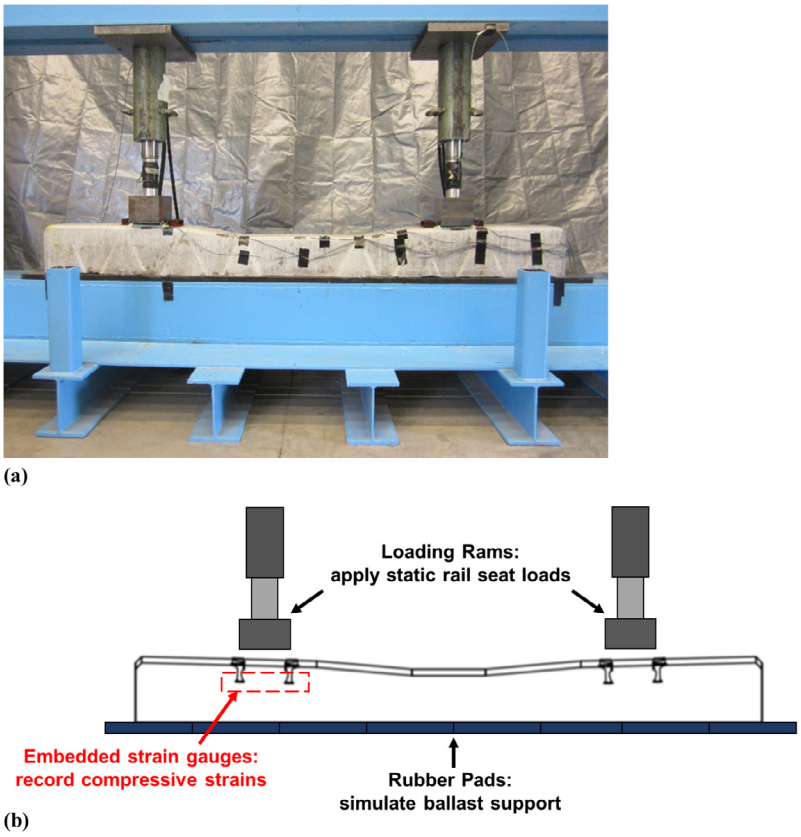

Fig. 9. Static Load Testing Machine (SLTM): (a) loading frame with the 102 in. (259 cm) long instrumented crosstie, (b) schematic drawing.

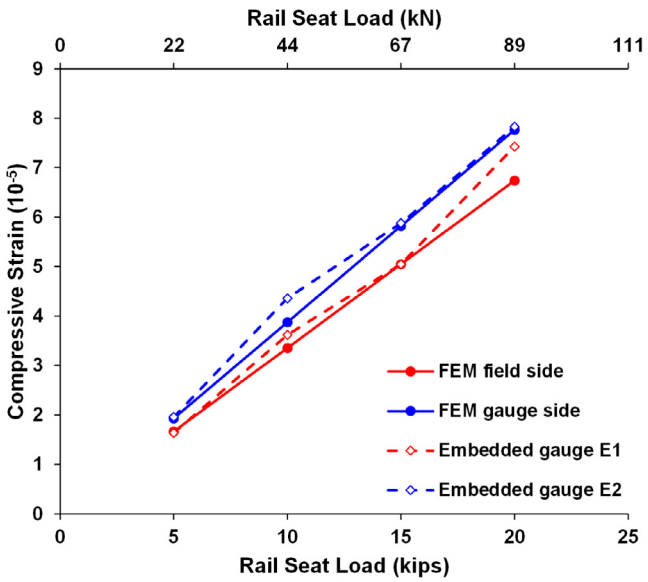

Fig. 10. Compressive strain comparisons between laboratory experimentation data and FE results.

culating concrete crosstie's flexural resistance [5]. In order to capture these two load values, a range of loads between 10 kip (44.5 kN) and 62.1 kip (276 kN) were selected for running the parametric study. By keeping the support condition constant, the direct relationship between the distribution angle and the rail seat load magnitude can be established. Therefore, all the loading scenarios were tested on the "full support" condition.

Fig. 11 shows the relation between distribution angle and rail seat load. As the rail seat load increased, the stress became more widely distributed within the prestressed concrete, and the distribution angles increased as well. When the rail seat load was 10 kip (44.5 kN), the distribution angle at the field side was 25.5 degrees. And when the seat load was 62.1 kip (276 kN), the high-impact load, the field side distribution angle was 36 degrees. As the rail seat load increased from 20 kip (89 kN) to 30 (133 kN) kips, the distribution angle at the field side (θ_f) stayed the same; as the rail seat load increased from 40 kip (178 kN) to 50 kip (222 kN), both angles (θ_f and θ_g) stayed the same. The possible reason for this insensitivity is that the angle increase within these load ranges was not great

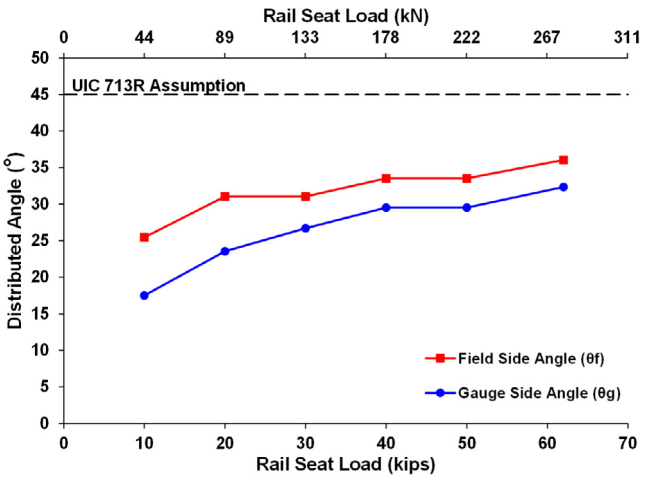

Fig. 11. Relation between distribution angles and rail seat loads.

enough to be captured by the model (less than 2.5 degrees). It should be noted that neither θ_f nor θ_g ever reached or exceeded the UIC assumed 45 degree assumption over the chosen load range (i.e. 95% of the field-detected rail seat loads).

Different from the assumptions made by UIC 713R, the distributed vertical load was not symmetric across the center line of rail seat, as the distribution angles, θ_f and θ_g, never had the same value. The asymmetry can most-likely be attributed to the cant of the rail seat regions. UIC 713R also assumes that the rail seat load is uniformly distributed along the neutral axis of the concrete crosstie. However, it can be clearly seen in Fig. 12 that even though the stress was spread out below the rail seat, the majority of the stress exerted on the neutral axis was concentrated about the center line of the rail seat. Because the compressive stress below the rail seat was neither 45-degree inclined nor uniformly distributed, the negative bending moment that the compressive stress induced should be less than what is suggested by UIC 713R. Since the positive moment induced by ballast stayed the same (assume uniform reaction force for both cases), the resultant positive rail seat moment according to FE modeling was greater than UIC 713R's recommendation. Therefore, the equation that UIC 713R uses to calculate the design rail seat positive bending moment should be considered as less conservative, as UIC 713R assumes the compressive stress to be spread over a greater length along the neutral-axis, leading to its overestimation of the negative bending moment induced by the compressive stress and its underestimation of the resultant rail seat bending moment. The authors believed that the accurate rail seat positive bending moment under a high-impact rail seat load of 62.1 kip (276 kN) should fall within the area between the blue and yellow curves shown in Fig. 3.

4.2. Effect of support condition on distribution angle

It has previously been documented that a concrete crosstie's flexural behavior is very sensitive to changes in support condition [5]. Understanding the stress distribution within the crosstie is essential to quantifying its flexural capacity. Previous research has been performed at RailTEC to measure a concrete crosstie's bending moments with five different support conditions [12]. The parametric study incorporated these support conditions, illustrated in Fig. 13, into analysis by assuming the geometry of the ballast was made of discrete rubber supports. Notice that the ballast support is shown as several shaded square bins, each of which is 12 in. (30.5 cm) by 12 in. (30.5 cm) in the FE model.

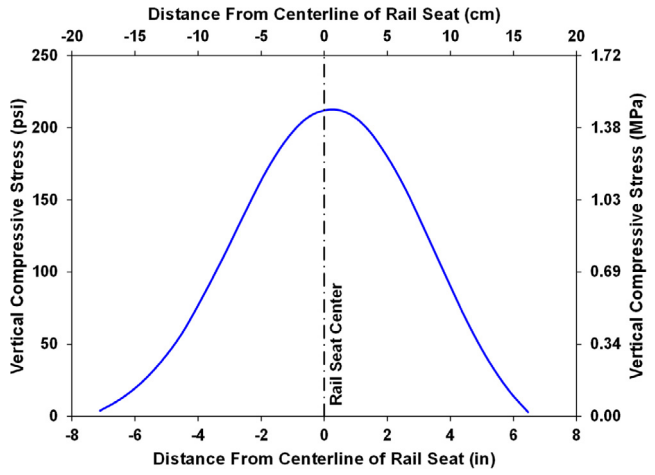

Fig. 12. Compressive stress distribution along the neutral axis under "full support" condition and 20 kip (89 kN) of rail seat loads.

Both 20 kip (89 kN) and 62.1 kip (276 kN) vertical rail seat loads were applied on the rail seats for each support conditions, so a total of 10 tests were conducted. For both of the applied loads, different support conditions were the only factor that could potentially affect the values of both distribution angles.

Table 3 provides a comparison of the values of distribution angles found in all 10 tests. As shown in the table, the support conditions affected the distribution angles in the same way for both load cases, that is, when the distribution angle increased from one support condition to another under the 20 kip (89 kN) rail seat load, the angle would also increase for the 62.1 kip (276 kN) rail seat load, and vice versa. The consistency between the two load cases indicated that changing the support conditions would alter the compressive stress distribution in certain ways, regardless of the magnitude of load applied at the rail seats. However, the sensitivity of load distribution to changes in support conditions depended on the magnitude of the rail seat loads, as the percent difference between angles of two support conditions did not stay the same for both load cases.

The stress distribution below the rail seats was impacted as the ballast reaction shifted toward the center region of the crosstie, as is evident from the results from the "light center binding" and "high center binding" support conditions (Fig. 13(b) and (c)). Specifically, as the support conditions moved from "full support" to "light center binding", both of the distribution angles increased, but as the support condition moved from "light center binding" to "high center binding", the distribution angles at the field side (θ_f) decreased to values that were lower than those under "full support", while the angles at the gauge side (θ_g) increased to almost 90 degrees. The dramatic change of stress distribution was possibly caused by the movement of ballast reaction. When the ballast was shifted towards the center, but the rail seat sections were still fully supported, the compressive stress at the field side tended to be distributed towards the end of the ballast, where the reaction force went to zero; meanwhile, the compressive stress at the gauge side was spread over a greater length to counter the concentrated reaction force at the center. The combination of these two stress behaviors led to an increase in both θ_f and θ_g. When the ballast reaction was concentrated at the center and the rail seat sections were no longer supported, most of the compressive stress was spread towards the center region, resulting in a decrease in θ_f and an increase in θ_g.

For "lack of rail seat support", both distribution angles decreased compared to those found in "full support", but the angles at the field side (θ_f) were exactly the same as those in "high center binding". This behavior corresponded closely with the hypothesized behavior referenced earlier. Given the rail seat sections were not supported in either the "lack of rail seat support" or "high center binding" cases, the compressive stress in the field side tended to be distributed narrowly. This narrow distribution resulted in the same distribution angles for both cases. However, the compressive stress in the gauge side could no longer reach the center ballast under "lack of rail seat support", as the concentrated ballast reaction in the center region was further away from the rail seat sections, thus leading to a decrease in θ_g.

It is noticeable that among all five support conditions, the angle difference between "full support" and "lack of center support" was the smallest, especially for θ_g in the 62 kip (276 kN) rail seat load case, in which there was only a 0.4-degree difference between the two support conditions. "Lack of center support" can also be considered as the newly tamped support condition. Based on the data measured from the previous laboratory testing, it was concluded that tamping at the rail seat sections is beneficial for crossties subject to center binding because it helps reduce the center negative bending moment experienced by the crosstie without changing the rail seat positive moment (or the changes are very

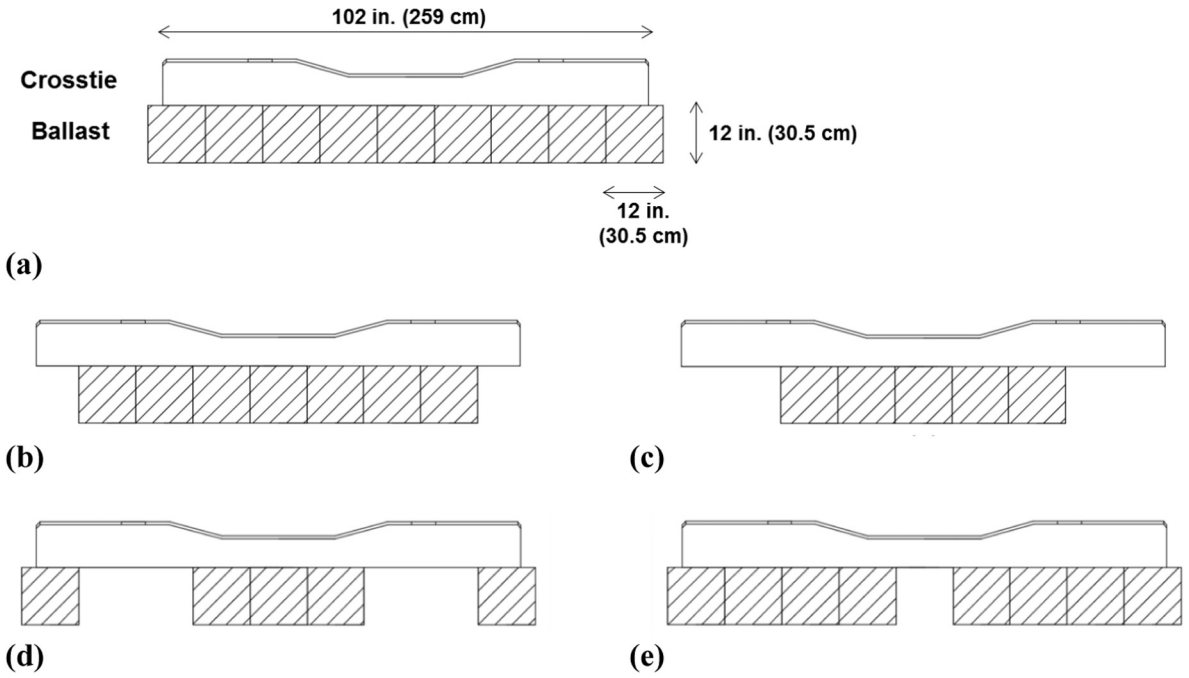

Fig. 13. Different support conditions: (a) full support, (b) light center binding, (c) high center binding, (d) lack of rail seat support, (e) lack of center support (12).

Table 3
Comparison of distribution angles in different support conditions.

Support Condition	20 kip (89 kN)		62.1 kip (276 kN)	
	Rail Seat Load		Rail Seat Load	
	θ_f (°)	θ_g (°)	θ_f (°)	θ_g (°)
Full Support	31.1	23.6	36.0	32.4
Light Center Binding	40.5	26.7	50.9	39.6
High Center Binding	28.3	–*	25.5	–*
Lack of Rail Seat Support	28.3	20.4	25.5	23.6
Lack of Center Support	33.5	26.7	38.3	32.8

* Note: the stress was spread too widely that the angle values were hard to be determined.

minimal) [12]. This behavior is consistent with the FE results. Even though there was a slight increase in the distribution angles from "full support" to "lack of center support", the effect of having a larger range of compressive stress distribution under "lack of center support" case could be countered by the more concentrated ballast reaction at the rail seat sections, thus it is highly possible that the rail seat positive bending moments between the two support conditions would stay the same.

Based on the results from the parametric study, one potential explanation of the rare occurrence of rail seat positive failures could be found in the nature of UIC 713R's design methodology. Since the design method is geometry-based, mainly depending on the depth of the rail seat sections, as long as manufacturers design the crossties with very deep rail seat sections, the design rail seat bending moment can be large enough that it will not be exceeded during the entire service life. Therefore, more field and laboratory data are needed to determine the maximum rail seat positive bending moment a crosstie can potentially experience, then design the geometry of the rail seat sections based on this value. For AREMA and AS, since load distribution below rail seats is not considered in their design methodologies, their design rail seat bending moments are overestimated, leading to over-designed rail seat sections. Reducing rail seat depths or rearranging the prestressing wires can potentially lower the flexural capacity at rail seat sections. However, continuation of this research project has to be done to be able to optimize the design methodology of concrete crossties.

5. Conclusions and discussions

AREMA, AS, and UIC all have different assumptions as how the rail seat load is transferred inside the concrete crosstie in their design methodologies. In order to better understand the load path going through prestressed concrete crosstie and investigate the vertical compressive stress distribution below the rail seats, a parametric study using three-dimensional FE modeling technique has been performed and the FE model used in this study was also validated through laboratory experiments. Several conclusions can be drawn based on the limited results from this study as follows:

FE results show that compressive stress is indeed distributed over the neutral axis of the concrete crosstie at certain angles. Under the same support condition, an increase in rail seat load magnitude could increase stress distribution angles on both field and gauge sides, and therefore increase the range in which the compressive stress is distributed over the neutral axis. Additionally, the distribution of stress below the rail seats was found to

be sensitive to varying support conditions. However, the distribution angles of the "full support" case and the "lack of center support" case were relatively similar, indicating the rail seat positive bending moments experienced by both cases would be similar as well.

The findings from this parametric study also suggest that some of the assumptions made by UIC 713R may not be applicable to all scenarios. To be more specific, UIC 713R assumes the stress to be uniformly distributed along the neutral axis of the crosstie at 45 degree angles at both field and gauge sides and the stress distribution was assumed to be symmetric along the center line of the rail seat. However, the findings from the parametric study indicate the compressive stress to be more concentrated about the center line of the rail seat, and under the support condition chosen by UIC 713R for calculating the design moment ("lack of center support"), both distribution angles were below 45 degrees, even when the high impact load was considered. In addition, the stress distribution was found to be asymmetrical (the percent difference between distribution angles at field and gauge sides ranges from 10% to 31%) in this study, likely due to rail seat cant. Those assumptions mentioned above could lead to less-conservative design of flexural strength at rail seat.

Acknowledgments

This research was funded by National University Rail (NURail) Center. The authors would like to express their gratitude to Zhe (George) Chen for providing the initial FE model for the parametric study. The authors would also like to thank Zhipeng Zhang for his assistance on creating the CAD drawings, Tom Roadcap and Josue Cesar Bastos for their assistance with laboratory experimentation. Henry E. Wolf has consistently provided feedback throughout the entire project. The authors appreciates Kaijun (Kevin) Zhu's tremendous help with refining the FE model and troubleshooting the errors occurred during the modeling process. J. Riley Edwards has been supported in part by grants to the UIUC Railroad Engineering Program from CN, Hanson Professional Services, and the George Krambles Transportation Scholarship Fund.

References

[1] W.W. Hay, Railroad Engineering, 2nd Ed., John Wiley and Sons, New York, 1983.
[2] M/W budgets to climb in 2008. Railway Track & Structures 2008 104(1) 18–25.
[3] D. Harris, R. Lutch, T. Ahlborn, P. Duong, Optimization of a prestressed concrete railroad crosstie for heavy-haul applications, J. Transp. Eng. 137 (11) (2011) 815–822.
[4] B.J. Van Dyk, Characterization of Loading Environment for Shared-Use Railway Superstructure in North America, M.S. Thesis, University of Illinois at Urbana-Champaign, Urbana, Illinois, 2013.
[5] H.E. Wolf, S. Mattson, J.R. Edwards, M.S. Dersch, C.P.L. Barkan, Flexural Analysis of Prestressed Concrete Monoblock Crossties: Comparison of Current Methodologies and Sensitivity to Support Conditions. In: Proceedings of Transportation Research Board 94th Annual Conference, Washington, D.C., January 2015.
[6] American Railway Engineering and Maintenance-of-Way Association, Manual for Railway Engineering, AREMA, Lanham, Maryland, 2014.
[7] Standards Australia International, AS 1085.14, Railway track material, part 14: prestressed concrete sleepers, 2003.
[8] International Union of Railways, UIC 713R, Design of monoblock concrete sleepers, 2004.
[9] Z. Chen, M.G. Shin, S. Wei, B. Andrawes. Finite Element Modeling and Validation of the Fastening System and Concrete Sleepers Used in North America, in: Proceedings of the Institution of Mechanical Engineers, Part F: Journal of Rail and Rapid Transit, April 2014.
[10] H. Yu, D. Jeong, J. Choros, T. Sussmann, Finite Element Modeling of Prestressed Concrete Crossties with Ballast and Subgrade Support, in: Proceedings of the ASME 2011 International Design Engineering Technical Conferences & Computers and Information in Engineering Conference IDETC/CIE 2011, Washington, DC, August 2011.
[11] Z. Chen, Mechanistic Analysis of Concrete Crosstie and Fastening System Using Field-Validated Finite Element Model PhD Dissertation, University of Illinois at Urbana-Champaign, Urbana, Illinois, 2015.
[12] J.C. Bastos, Analysis of the Performance and Failure of Railroad Concrete Crossties with Various Track Support Conditions M.S. Thesis, University of Illinois at Urbana-Champaign, Urbana, Illinois, 2016.
[13] R.D. Holtz, W.D. Kovacs, T.C. Sheahan, An Introduction to Geotechnical Engineering. 2nd Ed. PEARSON, 2011.
[14] S. Wei, D.A. Kuchma, J.R. Edwards, M.S. Dersch, R.G. Kernes. Gauging of Concrete Crossties to Investigate Load Path in Laboratory and Field Testing, in: Proceedings of the 2014 Joint Rail Conference, Colorado Springs, CO, April 2014.
[15] H.E. Wolf, Y. Qian, J.R. Edwards, M.S. Dersch, D.A. Lange, Temperature-induced curl behavior of prestressed concrete and its effect on railroad crossties, Constr. Build. Mater. 115 (2016) 319–326.